JOURNAL OF PROPULSION AND POWER
Vol. 17, No. 1, January–February 2001

Gun Interior Ballistic Performance with Ammonium Nitrate-Alcohol Propellants

Akihiro Sasoh,* Toshihiro Ogawa,† and Kazuyoshi Takayama‡
Institute of Fluid Science, Tohoku University, Sendai 980-8577, Japan
Kazunari Ikuta§
Japan Steel Works, Ltd., Tokyo 100, Japan
and
Nobuo Nagayasu¶ and Shinobu Ohtsubo**
Chugoku Kayaku Co. Ltd., Hiroshima 737-21, Japan

A new type of propellant, a mixture of ammonium nitrate and alcohol, was examined in ballistic experiments. With prilled ammonium nitrate and ethanol, increased ballistic performance was obtained for the maximum energy release conditions. From the measured chamber pressures and measured in-tube velocity profile, the location of energy release and pressure wave motions are documented. This propellant is characterized by low-product molecular mass, high-specific energy, and high flexibility in controlling its performance both by changing the type of alcohol and by varying the reactants' molar ratio.

Introduction

BALLISTIC range is an important device in aerospace studies. In particular, it is indispensable in on-ground super/hypersonic aerothermodynamic flight simulations because of significant levels of upstream conditions. In existing aeroballistic technologies, a two-stage light-gas gun is better than a single- stage gun on ballistic-range performance. However, a two-stage light-gas gun is a costly device, requires large storage, and has a complicated structure. Electrothermal guns and electrothermal-chemical guns use electrical power to energize the propellant and increase the range performance. However, because the energy conversion efficiency in those devices are still low at the current state of the art, they need a large electrical power storage/supply system, thereby not necessarily being suitable for laboratories that mainly deal with gasdynamics and/or chemical propellants. If the launch projectile speed readily equals 1.5 km/s and higher when using single-stage guns, this would become a useful application.

There are several items to examine for improving the performance of a single-stage gun, namely increased gun pressure, increased material strength, and improvement of gun propellant performance. The muzzle velocity may be increased with increased gun pressure. But, high-pressure operations are not suitable for launching projectiles that are often fragile and/or have sensitive payloads. Efforts for developing high-specific-strength materials for projectiles have been continuously made. Several of the authors have reported a newly-developed aluminum alloy for ram accelerator studies.[1] Another issue to consider is an understanding of propellant characteristics. Intensive studies have been conducted on the performance of black and smokeless powders.[2] Liquid propellants, for example, hydroxylammonium nitrate (HAN)-based monopropellants, have been so intensively studied that their characteristics are fairly understood and summarized in a textbook.[3]

Ammonium nitrate is widely used as a material of industrial explosives, although investigations on its application to gun ballistics have not yet been made. Ikuta[4] proposed that the mixture of ammonium nitrate and alcohol could be a high-performance propellant. For simplicity, this mixture will hereafter be referred to as ammonium nitrate-alcohol (ANA) propellant. An important point is that their product molecular mass can be lower than that of existing gun propellants. Sasoh et al.[5] experimentally validated that ANA was really operationable in a ballistic range. However, in the previous study, the ammonium nitrate (AN) was not prilled, exhibiting a moderate performance.

Here, by using prilled AN, the performance of ANA has been much improved. Results of parametric studies on its ballistic-range performance and related discussions are presented below.

Properties of ANA

In this study, ethanol is used as the alcohol. Under the standard condition, AN, NH_4NO_3, is solid and ethanol is liquid. The solubility of AN into ethanol is 2.5 wt% at the room temperature. In this study, the mass of AN is at least 175% of that of the alcohol. Although the solution is saturated, most of AN remains insoluble. In this mixture, AN acts as oxidizer; alcohol as fuel. The equation for a fundamental chemical reaction, from which only CO_2, N_2, H_2O, and H_2 are assumed to be produced, is expressed as follows[4]:

$$C_nH_{2n+1}OH + xNH_4NO_3 \rightarrow nCO_2 + xN_2 + (1 + 3x - 2n)H_2O + (3n - x)H_2 + Q \quad (1)$$

where Q designates the heat of decomposition.

For ethanol, $n = 2$. Based on Eq. (1), an oxygen balance happens with $x = 6$. If x is smaller, hydrogen is produced. Figure 1 shows computed equilibrium fractions of chemical species in ANA product as a function of x. The computation is done using Kihata-Hikita-Tanaka (KHT) code.[6] Mole fractions computed from Eq. (1) are also plotted for comparison. For $x \simeq 1$, Eq. (1) overestimates the production of H_2, underestimating that of H_2O. Also, without the production of CO being taken into account, the production of CO_2 is overestimated. The larger the value of x, the smaller the deviation of Eq. (1) from the equilibrium state in estimating major components' mole fractions becomes.

The corresponding heat of decomposition, impetus, and molecular mass are plotted in Fig. 2. For $x \simeq 1$, the hydrogen fraction is

Received 9 May 1999; presented as Paper 99-2917 at the AIAA/ASME/SAE/ASEE 35th Joint Propulsion Conference, Los Angeles, CA, 20–24 June 1999; revision received 28 October 1999; accepted for publication 30 October 1999.

*Associate Professor, Shock Wave Research Center, 2-1-1 Katahira. Associate Fellow AIAA.
†Technical Staff, Shock Wave Research Center, 2-1-1 Katahira.
‡Professor, Shock Wave Research Center, 2-1-1 Katahira. Senior Member AIAA.
§General Manager, Hibiya Mitsui Building, 1-2 Yurakucho 1-Chome, Chiyoda-ku.
¶Senior Staff, Etajima-cho, Aki-gun.
**Department Chief, Etajima-cho, Aki-gun.

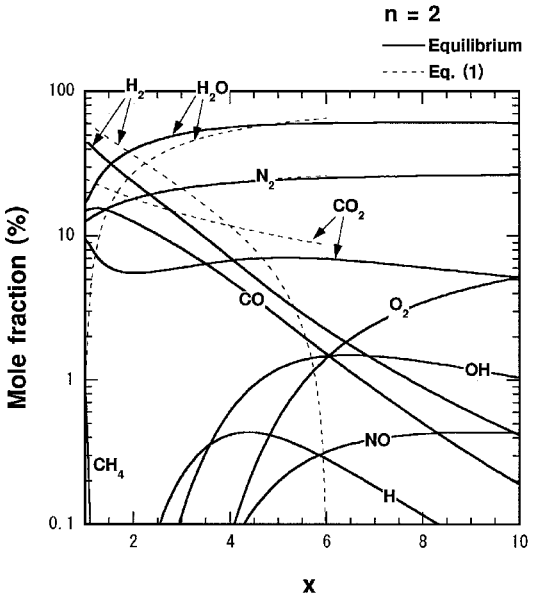

Fig. 1 Equilibrium chemical species fractions in ANA product as a function of x, computed with KHT code, $n = 2$.

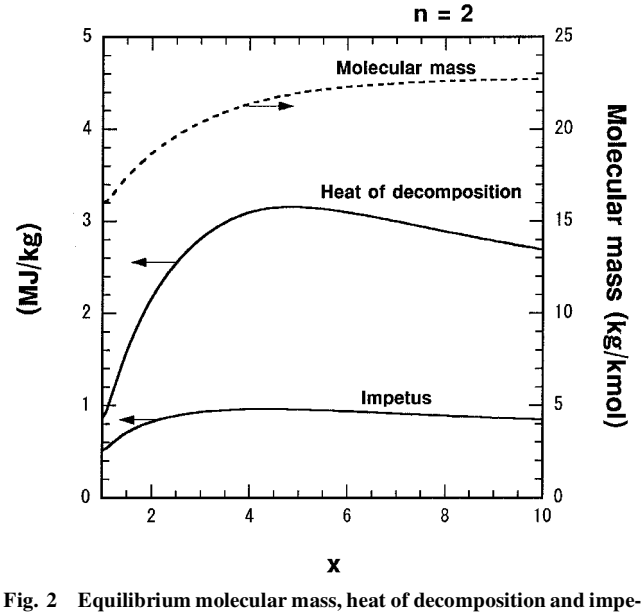

Fig. 2 Equilibrium molecular mass, heat of decomposition and impetus as functions of x, computed with KHT code, $n = 2$.

maximum. The molecular mass for $x = 1.0$ is as small as 16.0. This characteristic itself is desirable for high muzzle velocity operation. However, the heat of decomposition and impetus are considerably smaller.

The heat of decomposition is a maximum at 3.16 MJ/kg with $x = 4.7$. The product is composed mainly of H_2O, N_2, and CO_2. The mole fractions of H_2 and CO are lower than 5%. The mole fraction of H_2O (molecular mass; 18 kg/kmol) is 8.3 times higher than that of CO_2 (molecular mass; 44 kg/kmol). Therefore, the molecular mass is still at a low level, 21.8 kg/kmol.

Based on the computation, there are two operation regimes. For $x \simeq 1$, the main product is hydrogen molecule, and the product molecular mass and the heat of decomposition are relatively low. As previously stated, the heat of decomposition is highest for $x = 4.7$. Under this condition, the heat of decomposition is less sensitive to x, and the corresponding product molecular mass is still reasonably low.

These calculated equilibrium results may not necessarily apply directly to the evaluation of ballistic-range performance of ANA, and so experimental studies were carried out.

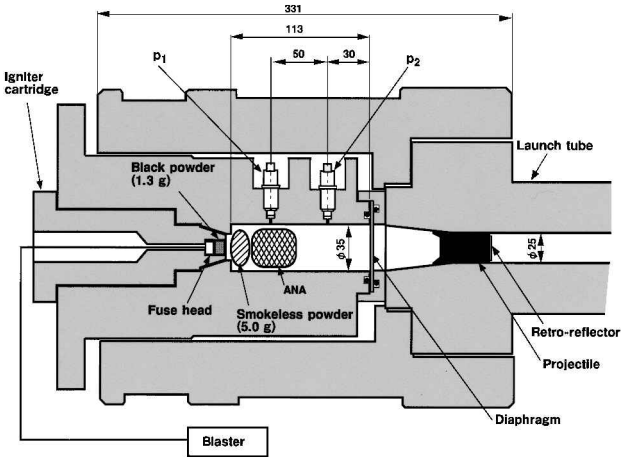

Fig. 3 Schematic illustration of propellant chamber.

Experimental Apparatus

The ballistic-range experiments were conducted using a single-stage gun. The bore diameter and the launch tube length are 25 mm and 2.0 m, respectively.[7] Figure 3 schematically illustrates its propellant chamber configuration. The propellant chamber inner shape is a 35-mm-diam, 113-mm-long cylinder. It is separated from the launch tube by a layer of stainless steel diaphragm (SUS304, 0.5 mm in thickness, with 0.2-mm-deep cross grooves). Its static rupture pressure was 20 MPa $\pm$ 15%. At the tip of the igniter cartridge, a fuse head is fabricated. It is surrounded by 1.3-g black powder. The igniter cartridge is set at the bottom of the propellant chamber. Being enclosed by tissue paper, 5.0-g smokeless powder (SP) (SS, Nippon Fat & Oil Co.) is loaded in front of the black powder. The amount of SP was sufficient for ignition with good repeatability. The reduction of SP amount was not explored in this study. The ANA is placed in front of the SP. It is packed in a 20-μm-thick polyethylene bag. The ethanol is saturated with ammonium nitrate. The ballistic performance was insensitive to mixing condition between these two substances. Even if the propellant was stored for 40 h, its ballistic performance did not change.

The propellant chamber and the launch tube are connected using a conical transition section. At the end of the transition section, a cylindrically-shaped projectile, made of high-density polyethylene (940 kg/m^3), is loaded. It has a Bridgman seal on its base, and its total length and mass are 40 mm and 16.2 g $\pm$ 0.5%, respectively.

To measure the time variation of propellant chamber pressures, two piezoelectric pressure transducers are recess-mounted. The response time of them is 1 μs. The spaces between the pressure transducers and the propellant chamber wall is filled with silicon grease. It was experimentally checked that the silicon grease did not affect the calibration of the pressure transducers and that the response time was sufficiently short for the present measurement. In this paper, the measured pressures are labeled p_1 and p_2, respectively, where p_1 is 80 mm and p_2 is 30 mm from the diaphragm (Fig. 3). The in-tube projectile velocity was measured using a velocity interferometer system for any reflector (VISAR). A 2-W argon ion laser was used as the light source. The incident light beam on the projectile is reflected from a layer of retro-reflector (3970G, 3M). The function of the retro-reflector is to reflect a light beam back in exactly the same direction as to the incident one itself. The reflected light is slightly diffused, but its intensity remained large enough for the VISAR measurement. For detailed description of VISAR and the present experimental set-up, see Refs. 8 and 9.

Results and Discussions

Basic Characteristics and Effect of Prilling

Basic characteristics and a necessary loading condition of ANA will be described first. Figure 4 shows time variations of p_1. Solid lines represent ones with ANA, the broken line without ANA. Two types of AN are examined here. One is prilled AN, which is

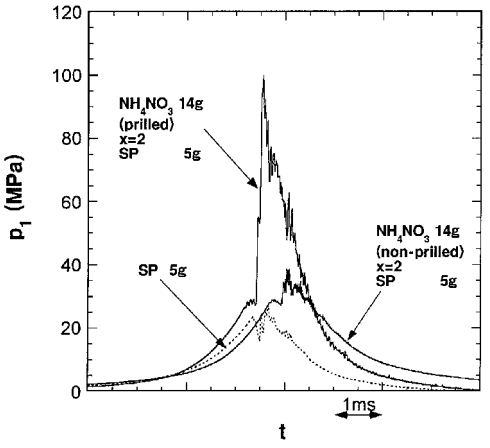

Fig. 4 Time variations of p_1, effect of AN and its condition.

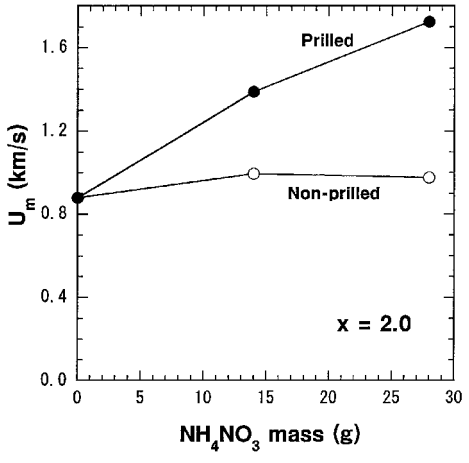

Fig. 5 Measured muzzle velocity, U_m, vs mass of AN, effect of AN condition. Error in U_m measurement is ± 2%.

composed of small spherical particles, having a diameter of the order of 1 mm. The particles have microscopic porous structure. Another one is nonprilled AN, which is composed of smaller, arbitrarily-shaped particles. The particles are highly hygroscopic and aggregation easily occur.

With only SP, p_1 first increases because of its combustion. A sudden pressure drop occurs when expansion waves generated by diaphragm rupture reaches the pressure measurement location. Following this pressure drop and with combustion of SP, p_1 again starts to increase, reaches a maximum and then decreases, because the expansion waves that are generated from the accelerating projectile propagate past the pressure measurement location.

With non-prilled AN, the rise rate of p_1 initially remains less than that without ANA. It is believed that the decomposition of the nonprilled AN and subsequent reactions with the ethanol are delayed, and that some portion of heat released from SP is spent to heat up the ANA, and the heat is lost to the propellant chamber wall. The peak value of p_1 in the present case is about 1.5 times larger than that without ANA.

When prilled AN is used, much higher peak pressures are observed. The peak value is 100 MPa and is 2.6 times larger than that with nonprilled AN. In this case, the pressure-rise rate is also higher than that without ANA even before the diaphragm rupture. The pressure did not drop even with the diaphragm rupture, and abruptly increased.

The above pressure profiles were reflected in the muzzle-velocity performance as shown in Fig. 5. Without ANA, a muzzle velocity of 0.88 km/s was obtained. On one hand, with nonprilled AN, the muzzle velocity U_m is insensitive to the amount of ANA. In this case, we believe that the combustion is incomplete during the projectile acceleration process. The energy gain is canceled by an increase in propellant mass. On the other hand, with prilled ANA, U_m becomes

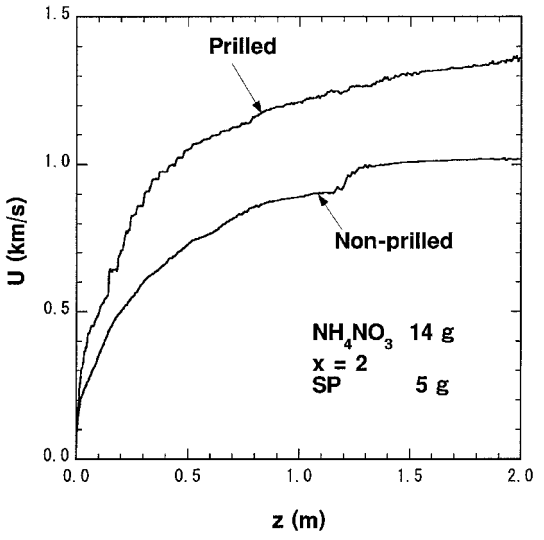

Fig. 6 Measured in-tube velocity profiles, effect of AN condition. z; projectile travel distance.

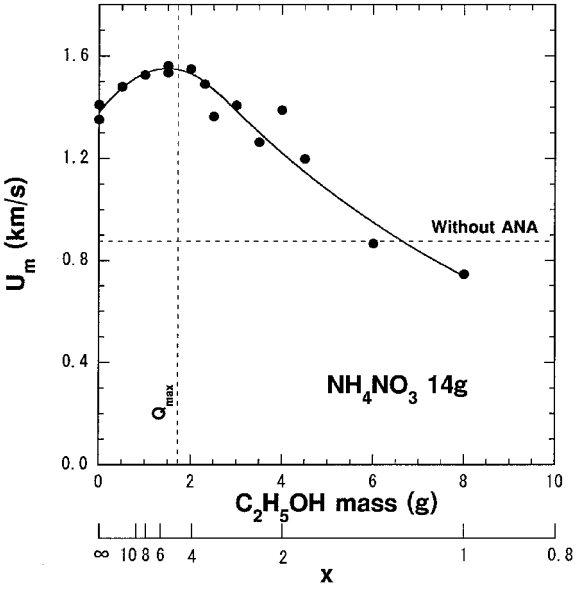

Fig. 7 U_m vs x, prilled AN. Error in U_m measurement is ± 2%.

an increasing function of the mass of the propellant. A muzzle velocity of 1.72 km/s was obtained with 28-g AN and 8-g ethanol. In operations for even higher muzzle velocities, the projectile could not remain intact. Therefore, in the present study, the muzzle velocity was limited to this level.

Figure 6 shows measured in-tube velocity profiles. With non-prilled AN, the velocity was almost constant in $z > 1.3$ m. However, with prilled-AN, the velocity continued to increase down to the muzzle. It follows from these results that much better ballistic performance is obtained with prilled AN. Therefore, in the following sections, only prilled AN is used; AN will implicitly designate prilled one.

Effect of Mixture Ratio

As shown in Eq. (1), for ethanol, the oxygen balances with $x = 6$; but as shown in Fig. 2, the equilibrium heat of decomposition has a maximum at $x = 4.7$. In Fig. 7, experimentally-measured muzzle velocities as a function of the mass of ethanol are plotted. The mass of prilled AN is kept constant, 14 g. To evaluate the oxygen balance, x is plotted along the abscissa. The muzzle velocity U_m has a maximum with ethanol mass around 1.5–2.0 g. The corresponding x ranges from 4.0 to 5.4. Therefore, with the resolution of x in the present experiments, this x range well corresponds to the condition

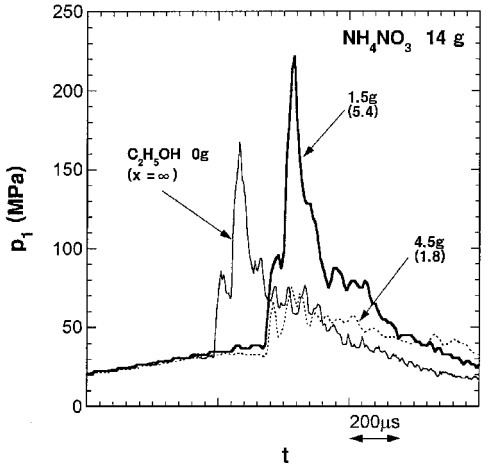

Fig. 8 Time variations of p_1 with different x, prilled AN.

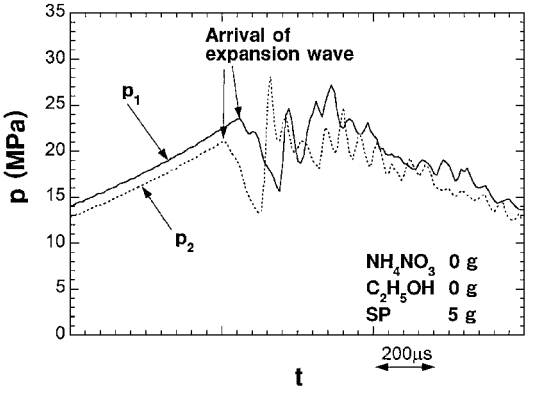

Fig. 9 Time variation of p_1 and p_2 with only SP.

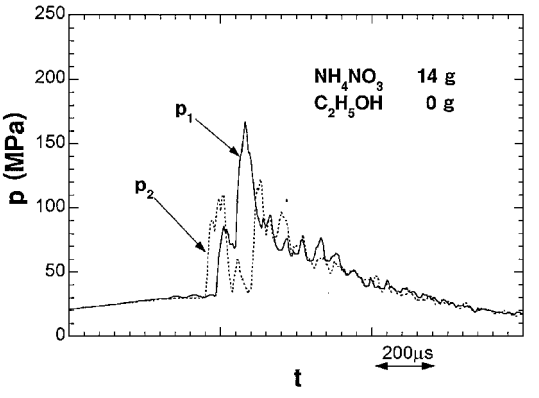

a) Ethanol 0 g

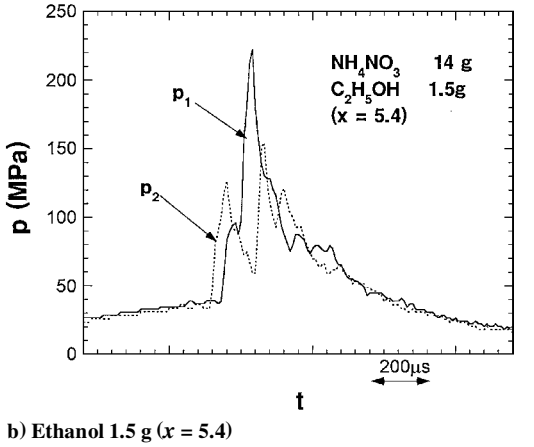

b) Ethanol 1.5 g (x = 5.4)

Fig. 10 Time variations of p_1 and p_2 with ANA and 5 g SP, prilled AN.

that the heat of decomposition has a maximum, which is labeled by Q_{max} in Fig. 7.

For small amounts of ethanol up to 2 g, the scatter in U_m is relatively small. In such conditions, the ethanol appeared well distributed in the porous AN particles. However, with larger amounts of ethanol (for $x \leq 3$), most portions of ethanol remained separated from AN, and as shown in Fig. 7, the scatter in U_m was large. With an ethanol mass of 6 g and larger ($x < 1.3$), U_m was actually less than that without ANA. This, again, is believed to be caused by incomplete combustion during the acceleration process.

The measured propellant chamber pressure variations (Fig. 8) are consistent with the muzzle velocity performance. With 1.5-g ethanol ($x = 5.4$), the peak value of p_1 was about 30% higher than that without ethanol. With 4.5-g ethanol ($x = 1.8$), the pressure level was much lower than the others.

Wave Motions in Propellant Chamber

Figure 9 shows time variation of p_1 and p_2 with only SP. As shown in Fig. 3, the location of p_1 is closer to the igniter cartridge by 50 mm than that of p_2. In this case, p_1 rises slightly earlier than p_2 does. Because the expansion waves generated by the diaphragm rupture reaches p_2 first, it starts decreasing earlier by 40 μs than p_1 does. These tendencies always appeared in ballistic experiments conducted by the authors with smokeless powders or a liquid propellant LP1846 [60.8% hydroxylammonium nitrate (HAN), 19.2% triethanolammonium nitrate (TEAN), and 20.0% H_2O].[7] In those cases, the propellants mainly got ignited near the igniter cartridge, because the compression waves generated by the ignited propellant propagated downstream, that is, in the direction from p_1 to p_2. Following the diaphragm rupture, expansion waves propagate upstream.

When testing ANA, the propellant chamber pressures exhibited peculiar characteristics. Figures 10a and 10b show time variations of propellant chamber pressures p_1 and p_2 with only prilled AN and with ANA propellant, respectively. Before pressure spikes appear, p_1 and p_2 gradually increase because of the combustion of SP, reaching about 30 MPa. These pressure-rise rates are consistent with those measured only with SP (Figs. 4 and 9). Note here that only with ANA pressure spike appears first in p_2 (downstream). After 35 μs, a pressure spike in p_1 (upstream) appears. The first peak value is lower in p_1 than p_2. The pressure p_2 sharply decreases after its first peak; this is believed to be caused by the expansion waves generated by the diaphragm rupture.

Comparing Figs. 9 and 10b, the characteristics in the propellant chamber pressures with ANA are interpreted in the following way: Because the ignition delay time of ANA is relatively long, initially the propellant is mechanically blown toward downstream and hits the diaphragm. Following this movement, the ANA gets ignited, generating compression waves. The compression waves coalesce to form a shock wave, propagating upstream. The velocity of this shock wave is estimated to be 1.4 km/s (Fig. 10b). According to the KHT code, C-J detonation velocity of this ANA in its condensed phase is calculated to be 7.7 km/s. Therefore, this observed wave is a combustion-driven gaseous shock wave. The shock wave is reflected from the igniter cartridge and propagate downstream. The second pressure spike in p_1 is caused by the reflected shock wave passing over. The reflected shock wave reaches the location of p_2 after the expansion waves passed there. Hence, the peak value of the second pressure spike is much lower there than that in p_1.

Gun Propellant Performance

In the present experiments, a maximum ballistic efficiency of 0.28 was obtained with prilled AN of 14 g and ethanol of 1.5 g ($x = 5.4$, $U_m = 1.56$ km/s). In calculating the ballistic efficiency, energies released both from ANA and the SP are taken into account. Although this value is already at a reasonably-high level, there may be a possibility of further improving the ballistic performance.

Figures 11a and 11b show projectile acceleration profiles. A projectile travel distance is designated by z. The acceleration is

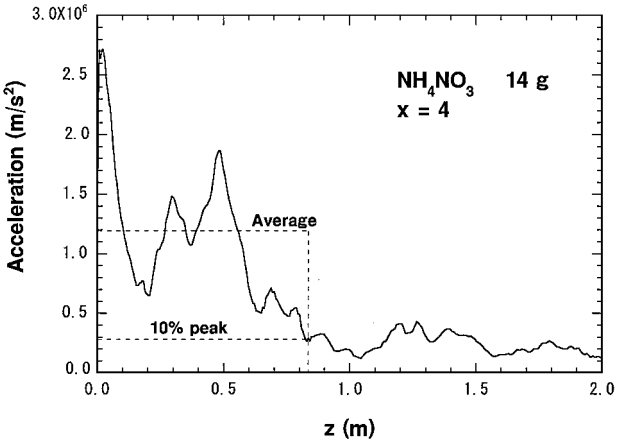

a) Ethanol 2 g ($x = 4.0$), $U_m = 1.56$ km/s

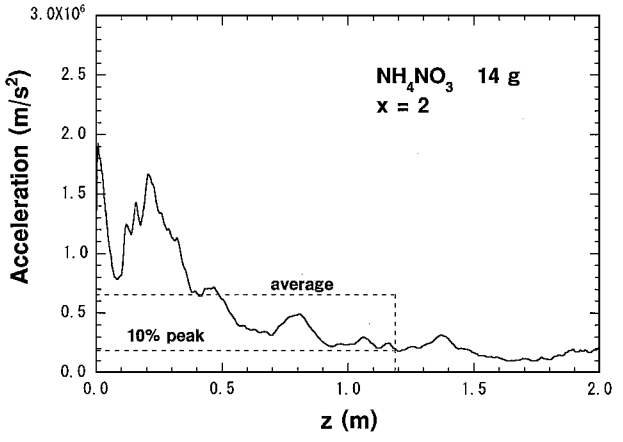

b) Ethanol of 4 g ($x = 2.0$), $U_m = 1.39$ km/s, prilled AN

Fig. 11 Projectile acceleration profiles.

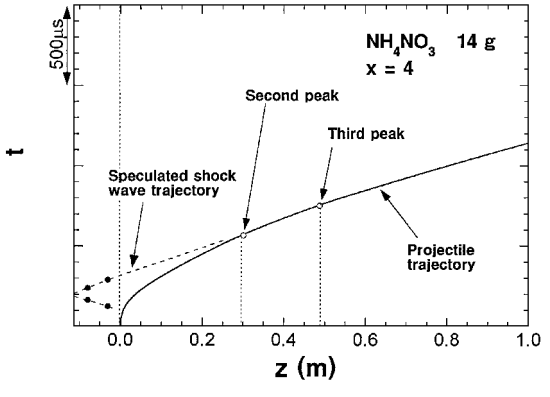

Fig. 12 z-t trajectories of projectile and shock waves, ethanol 2 g (x = 4.0), prilled AN, closed circle; pressure peak in propellant chamber.

estimated by a smoothed value of $U(dU/dz)$, where U is measured using the VISAR, and dU/dz is evaluated by numerically differentiating the U variation. The operating condition of Fig. 11a corresponds to the best performance within the framework of this study. Immediately following the diaphragm rupture, the acceleration is maximum. The second and third peak in the acceleration appear at $z = 0.30$ and 0.49 m, respectively. As shown in Fig. 12, it is speculated that those peaks are originated in the reflected shock waves in the propellant chamber (Fig. 10b). The location of these peaks depends on the relation between the projectile and shock wave motions. When the initial projectile acceleration is lower (Fig. 11b), the second peak appears at a location much closer to the diaphragm ($z = 0.21$ m).

With the plural acceleration peaks, the piezometric efficiency in the operations of Figs. 11a and 11b are fairly high. The piezometric efficiency is defined as an average-to-peak ratio in an acceleration profile. The average value of the acceleration is given by dividing the integration of an acceleration profile from $z = 0$ to the location where the acceleration becomes 10% of the peak value by the distance between the two locations (Figs. 11a and 11b). The piezometric efficiencies thus calculated equals 0.41 for Fig. 11a and 0.38 for Fig. 11b, respectively.

From Fig. 2, the molecular mass of the product under the condition of Fig. 11a equals 22.1 kg/kmol. With this reasonably low value, this propellant is suitable for high-muzzle-velocity operation. By increasing the projectile acceleration, the location where high acceleration is obtained by the reflected shock wave is expected to shift downstream, and the work done by the propulsive force will be done more efficiently; the piezometric efficiency can be further improved. Unfortunately, in the present study, the peak acceleration was limited from mechanical strength of the projectile. Operation experiments in even higher muzzle velocity regime warrant further efforts.

Conclusions

Experiments showed that mixtures of ANA resulted in a reasonably high-ballistic performance even in the moderate-scale facility. To increase the muzzle velocity, usage of prilled AN is necessary. With ethanol, the muzzle velocity became highest under the maximum heat of decomposition condition. Excessive amounts of ethanol resulted in incomplete combustion and, hence, in degradation of the ballistic performance. Because the products of ANA have low molecular mass and the heat of decomposition is reasonably large, this propellant proved to be suitable for high-muzzle-velocity operation. Having two independent parameters, n and x, controlling the propellant characteristics is possible in high flexibility. Considering that the sensitivity and toxicity of this propellant are low, and that its compositions are widely available with low cost, it is concluded that ANA can be competitive with, or even better than, other existing single-stage gun propellants. Further investigations are necessary for decreasing the ignition energy as well as exploring for even higher ballistic performance.

Acknowledgments

The authors are grateful to K. Tanaka with National Institute of Materials and Chemical Research, Tsukuba, Japan, for his offering KHT code usage to us. We also appreciate technical supports from Y. Mizuno, graduate student of Tohoku University, H. Ojima, M. Kato, K. Asano with Institute of Fluid Science, and S. Nakamura with Japan Steel Work Ltd.

References

[1] Sasoh, A., Hamate, Y., and Takayama, K., "Significance of Unsteadiness in Operation of the Small Bore Ram Accelerator," AIAA Paper 98-3446, July 1998.

[2] Stiefel, L. (ed.), *Gun Propulsion Technology,* Progress in Astronautics and Aeronautics, Vol. 109, AIAA, New York, 1988, Chaps. 2, 5, 13, 14.

[3] Klingenberg, G., Knapton, J. D., Morrison, W. F., and Wern, G. P. (eds.), *Liquid Propellant Gun Technology,* Progress in Astronautics and Aeronautics, Vol. 175, AIAA, Washington, DC, 1997, Chaps. 1–5.

[4] Ikuta, K., "Ohmic Ignition of Alcohol-Ammonium Nitrate Mixture for Hot Light Gas Generation," *Japanese Journal of Applied Physics*, Vol. 36, Pt. 2, 1997, pp. L1413, L1414.

[5] Sasoh, A., Ogawa, T., and Takayama, K., "Use of Ammonium Nitrate-Alcohol (ANA) for Ballistic Range Propellant," *Shock Waves*, Vol. 9, No. 4, 1999, pp. 291–294.

[6] Tanaka, K., "Detonation Properties of High Explosives Calculated by Revised Kihara-Hikita Equation of State," *Eighth Symposium (International) on Detonation*, NSWC MP, Albuquerque, NM, 1985, pp. 86–194.

[7] Sasoh, A., Ohba, S., and Takayama, K., "Investigation on Utilization of Liquid Propellant in Ballistic Range Experiments," *Journal of the Japan Explosives Society*, Vol. 60, No. 5, 1999, pp. 205–211.

[8] Barker, L. M., and Hollenbach, R. E., "Laser Interferometer for Measuring High Velocities of Any Reflecting Surface," *Journal of Applied Physics*, Vol. 43, No. 11, 1972, pp. 4669–4675.

[9] Munson, D. E., and May, R. P., "Interior Ballistics of a Two-Stage Light Gas Gun Using Velocity Interferometry," *AIAA Journal*, Vol. 14, No. 2, 1976, pp. 235–242.